RSC Advances

PAPER

View Article Online
View Journal | View Issue

Cite this: *RSC Adv.*, 2023, **13**, 19695

Exploring novel aryl/heteroaryl-isosteres of phenylthiazole against multidrug-resistant bacteria†

Mariam Omara,[a] Mohamed Hagras, *[b] Mohamed M. Elsebaie, [b] Nader S. Abutaleb,[cd] Hanzada T. Nour El-Din, [e] Maria O. Mekhail, [f] Ahmed S. Attia,[eg] Mohamed N. Seleem,[ch] Marwa T. Sarg[a] and Abdelrahman S. Mayhoub[bi]

Antimicrobial resistance has become a concern as a worldwide threat. A novel scaffold of phenylthiazoles was recently evaluated against multidrug-resistant *Staphylococci* to control the emergence and spread of antimicrobial resistance, showing good results. Several structural modifications are needed based on the structure–activity relationships (SARs) of this new antibiotic class. Previous studies revealed the existence of two key structural features essential for the antibacterial activity, the guanidine head and lipophilic tail. In this study, a new series of twenty-three phenylthiazole derivatives were synthesized utilizing the Suzuki coupling reaction to explore the lipophilic part. The *in vitro* antibacterial activity was evaluated against a range of clinical isolates. The three most promising compounds, **7d**, **15d** and **17d**, with potent MIC values against MRSA USA300 were selected for further antimicrobial evaluation. The tested compounds exhibited potent results against the tested MSSA, MRSA, and VRSA strains (concentration: 0.5 to 4 μg mL^{-1}). Compound **15d** inhibited MRSA USA400 at a concentration of 0.5 μg mL^{-1} (one-fold more potent than vancomycin) and showed low MIC values against ten clinical isolates, including linezolid-resistant strain MRSA NRS119 and three vancomycin-resistant isolates VRSA 9/10/12. Moreover, compound **15d** retained its potent antibacterial activity using the *in vivo* model by the burden reduction of MRSA USA300 in skin-infected mice. The tested compounds also showed good toxicity profiles and were found to be highly tolerable to Caco-2 cells at concentrations of up to 16 μg mL^{-1}, with 100% of the cells remaining viable.

Received 26th April 2023
Accepted 12th June 2023

DOI: 10.1039/d3ra02778c

rsc.li/rsc-advances

1. Introduction

Antimicrobial resistance (AMR) has recently become one of the most significant worldwide threats and has acquired an obvious priority status in global public health.[1] Mainly, the combination of antibiotics overuse and the slow discovery of new antibiotics has led to the increase in the incidence of AMR *via* stimulation of bacterial natural defense mechanisms, such as point mutations, bacterial evolution, and horizontal resistance gene transfer.[2] In the United States, annual reports have referred to millions of resistant infections with more than 35 000 deaths.[3] In addition, the pandemic COVID-19 is expected to increase AMR development as 70% of COVID-19 patients use antibiotics.[4,5] The adverse effects of AMR are not limited to health problems, as it clearly has an influence on the global economy where billions of USD have been spent for the sake of treating resistant bacterial infections.[6] According to the World Health Organization (WHO) priority pathogen list, both methicillin-resistant and vancomycin-intermediate or – resistant *Staphylococcus aureus* (MRSA, VISA and VRSA, respectively) are categorized as high priorities.[7] Methicillin-resistant *S. aureus* (MRSA)

[a]*Department of Pharmaceutical Organic Chemistry, College of Pharmacy (Girls), Al-Azhar University, Cairo, Egypt*
[b]*Department of Pharmaceutical Organic Chemistry, College of Pharmacy (Boys), Al-Azhar University, Cairo 11884, Egypt. E-mail: m.hagrs@azhar.edu.eg*
[c]*Department of Biomedical Sciences and Pathobiology, Virginia-Maryland College of Veterinary Medicine, Virginia Polytechnic Institute and State University, Blacksburg, Virginia 24061, USA*
[d]*Department of Microbiology and Immunology, Faculty of Pharmacy, Zagazig University, Zagazig 44519, Egypt*
[e]*Department of Microbiology and Immunology, Faculty of Pharmacy, Cairo University, Cairo 11562, Egypt*
[f]*PharmD-Clinical Pharmacy Undergraduate Program, Faculty of Pharmacy, Cairo University, Cairo 11562, Egypt*
[g]*Department of Microbiology and Immunology, School of Pharmacy, Newgiza University, Giza, Egypt*
[h]*Center for One Health Research, Virginia Polytechnic Institute and State University, Blacksburg, Virginia 24061, USA*
[i]*Nanoscience Program, University of Science and Technology, Zewail City of Science and Technology, Giza, Egypt*

† Electronic supplementary information (ESI) available. See DOI: https://doi.org/10.1039/d3ra02778c

is a major cause of nosocomial and community-acquired infections worldwide.[8] MRSA is resistant to most traditional antibiotics, such as β-lactams, fluoroquinolones, aminoglycosides, and tetracyclines.[9–13] Furthermore, MRSA has developed resistance against vancomycin and linezolid, the drugs of choice for treatment against it. Thus, there is an urgent need to develop new effective antimicrobial agents.[14–16]

Previously, a novel antibacterial scaffold was discovered by our research group containing *n*-butylphenylthiazole (**I**) (Fig. 1). It showed a MIC value of 4.8 μg mL^{-1} against MRSA and was considered as a lead compound for further development. The lead **I** has two essential features: a lipophilic moiety (blue color, Fig. 1) and a cationic moiety (red color, Fig. 1). During the optimization of the lead compound, the replacement of the *n*-butyl group with a phenyl ring (**II**) decreased the MIC value to 2.4 μg mL^{-1} (Fig. 1).[17] Meanwhile, rigidification by acetylene linked to a heteroaromatic system (**III**) afforded an improvement of the antibacterial activity (MIC = 2 μg mL^{-1}).[18] In this study, we aim to further advance the lead developments based on the previous results by utilizing two new lead optimization strategies: scaffold simplification and bioisosteric replacement techniques to develop novel and potent derivatives. Furthermore, we aim to investigate the structure–activity relationship of novel phenylthiazoles using the Suzuki–Miyaura coupling reaction (Fig. 1).[19–24]

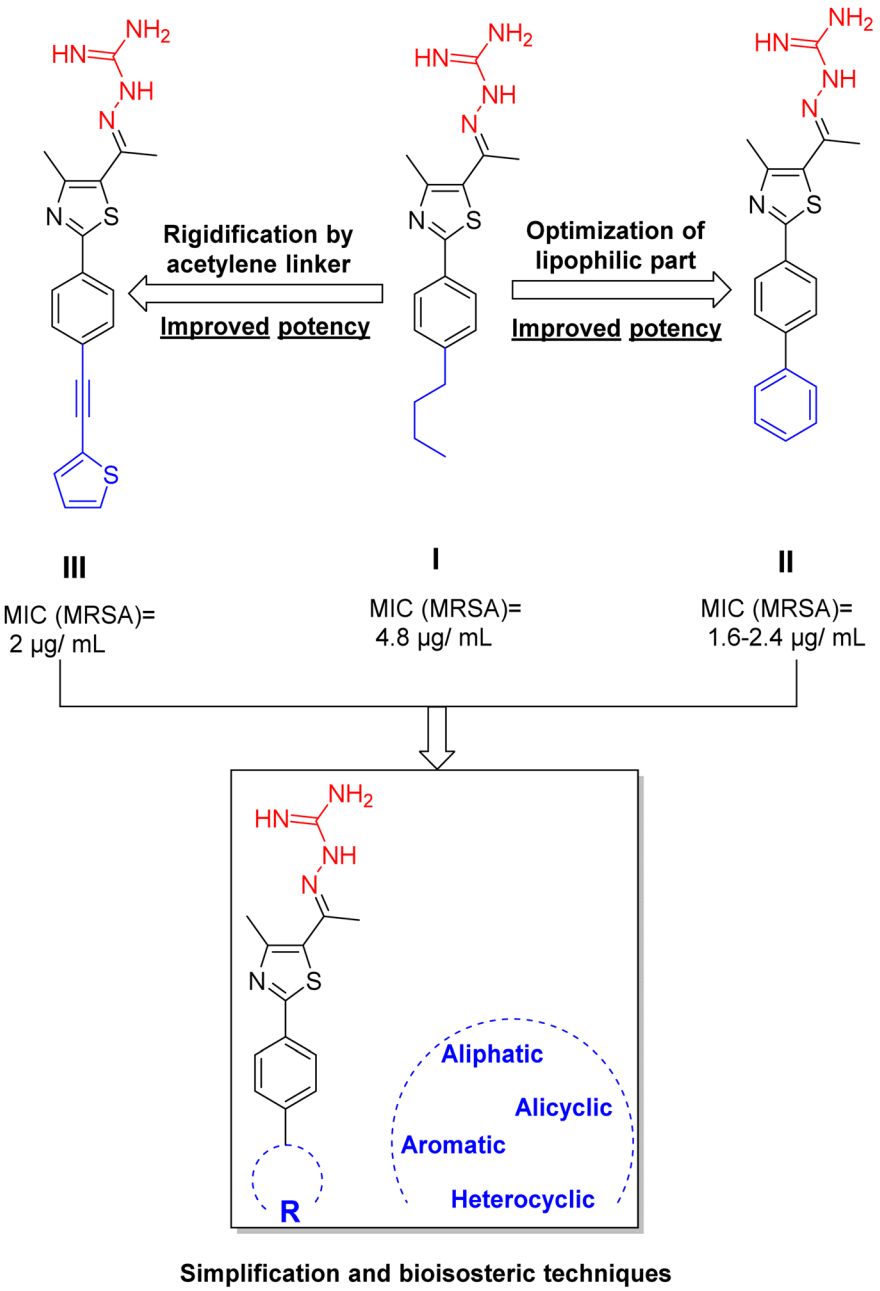

Fig. 1 The design of the current study based on the previous study.

2. Results and discussion

2.1. Chemistry

Hantzsch thiazole synthesis between 4-halobenzothioamide (**1a,b**) and α-chloroacetylacetone afforded the key starting material phenylthiazole (**2a,b**).[18,25] The alkyl and aryl derivatives were introduced using typical Suzuki cross-coupling conditions, as mentioned in Scheme 1, *via* two synthetic routes. The first one involved the direct reaction of boronic acid derivatives with *p*-iodophenylthiazole in one step.[22] The second method is an *in situ* borylation of *p*-chlorophenylthiazole, followed by reaction with the second aryl halide, which was suitable for a wide range of derivatives (Table 1).[26] Thiophene sulfonamide derivatives **19–25** were synthesized *via* nucleophilic substitution reaction of the corresponding sulfonyl chloride with proper amines in the presence of triethylamine.[27] Finally, aminoguanidine derivatives (**3–25d**) were obtained through condensation between **3–25c** with aminoguanidine HCl in the presence of a catalytic amount of hydrochloric acid (Scheme 1).

2.2. Biological evaluation

2.2.1. Initial antimicrobial screening. All final products were subjected to initial screening against MRSA USA300 (Table 2). Aliphatic and alicyclic derivatives **3d** and **4d** showed moderate and weak activity (MIC = 8 and 32 μg mL^{-1}, respectively). On the other hand, the phenyl-containing derivatives **5d–9d** were more potent, with MIC values ranging between 2–8 μg mL^{-1}. Changing the positions of the methyl group from para **5d** to meta **6d** led to a decrease in the activity by one-fold. Meanwhile, for the methoxy group containing compounds **7d** and **8d**, the activity was retained with MIC = 2 μg mL^{-1}. The bulky substituent, methyl ester **9d**, was less active with MIC = 8 μg mL^{-1}. Also, the fused bicyclic compounds showed reasonable activity with MIC = 4 μg mL^{-1} for 2-naphthyl **10d** and weak activity (32 μg mL^{-1}) for both benzofuran **11d** and benzothiophene **12d**. Five-membered heteroaromatic compounds, furan, and thiophene, were evaluated with different positions and substitutions to expand the SAR study. The 2-furan **13d** derivative showed a drop in the anti-MRSA activity with MIC = 64 μg mL^{-1}, while the 3-furan derivative **14d** was 32 times more potent with MIC = 2 μg mL^{-1}. Replacement of furan with its bioisostere thiophene positively increased the activity as 2-thienyl derivative **15d** was equipotent to Vancomycin with MIC = 1 μg mL^{-1}. Shifting from 2-thienyl to 3-thienyl derivative **16d** decreased the activity to 4 μg mL^{-1}. Then, derivatization of the thiophene with a methyl group (**17d** and **18d**) resulted in deterioration of the activity in a direct proportional manner with the number of methyl group **17d** and **18d** (MIC = 2 and 4 μg mL^{-1}, respectively). Encouraged by the MIC obtained with the 2-substituted thiophene derivative **15d** (MIC = 1 μg mL^{-1}), we extended the length of the side chain *via* synthesis of a series of alkyl sulphonamide derivatives **19d–25d**. Unfortunately, sulfonamides **19d–25d** were moderately active with the MIC range between 16–32 μg mL^{-1}. To summarize the structure activity relationship, the cyclopropyl derivative with 3 carbon atoms showed weak activity, while the branched isobutyl

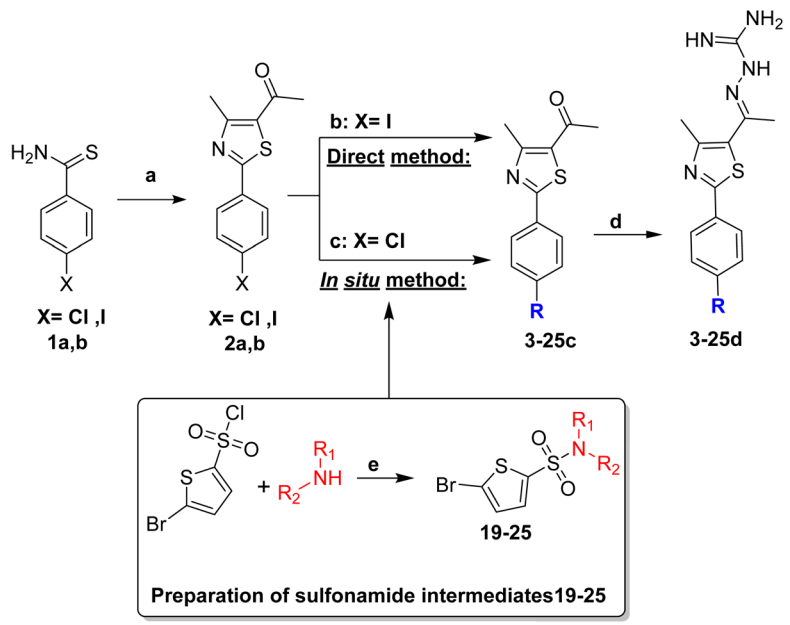

Reagents and conditions: **(a)** EtOH, 3-Chloro-2,4-pentanedione 6 h. reflux **(b)** **Direct method:** $Pd(OAc)_2$ (10% mol), X-Phos (20% mol), Cs_2CO_3 (2 equiv.), boronic acid derivatives, dioxan,180 °C for 24 h. **(c)** ***In situ* method:** 1 mol % of XPhos-Pd-G2, 2 mol % of XPhos, 3.0 equiv of NaOAc, 3.0 equiv of $B_2(OH)_4$, EtOH (0.1 M), 80 °C for 30 min. followed by addition of 3 equiv of 1.8 M K_2CO_3, 1 equiv of second halide or prepared sulfonamide intermediates,80 °C, 2 h., MW. **(d)** aminoguanidine HCl, Conc. HCl, EtOH, reflux. **(e)** triethylamine, DCM, 20 °C for 1 h.

Scheme 1

Table 1 Final products, compounds **3c,d–25c,d** obtained from Scheme 1

Compound number	R	Compound number	R
3c,d[a]		**15c,d**	
4c,d[a]		**16c,d**	
5c,d[a]	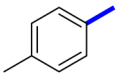	**17c,d**	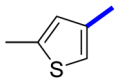
6c,d[a]	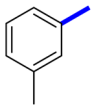	**18c,d**	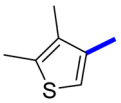
7c,d	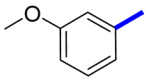	**19c,d**	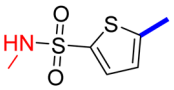
8c,d	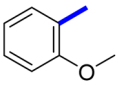	**20c,d**	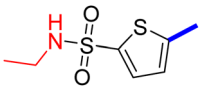
9c,d	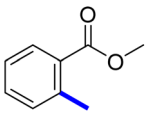	**21c,d**	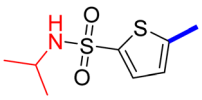
10c,d[a]	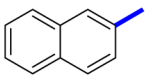	**22c,d**	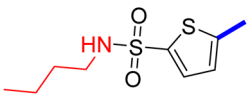
11c,d[a]	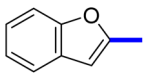	**23c,d**	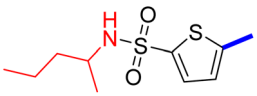
12c,d[a]	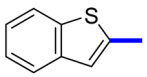	**24c,d**	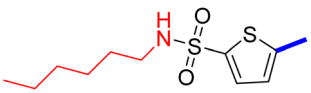
13c,d[a]		**25c,d**	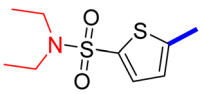
14c,d[a]			

[a] Compound synthesized *via* direct method (b).

derivative with 4 carbon atoms provided moderate activity. In the case of the phenyl derivatives, the insertion of a small polar substituent (*i.e.*, methoxy group) showed the upper hand over both a bulk polar ester and a nonpolar methyl group regardless of the substituent's position. In the fused system, the naphthyl derivative was more active than the fused heteroaromatic rings. Using 5-membered ring heterocycles leads to a variety of activities based on the position and substitutions on the ring. In the case of the furan side chain, the 2-furan derivative showed a drop in activity, while the 3-furan derivative was 32 times more potent. In contrast, 2-thiophene was the most active one, and the changing of the position or substitutions leads to a deterioration of the activity.

2.2.2. Profiling of antibacterial activity. Based on the initial screening results, the three compounds (**7d**, **15d** and **17d**) with MIC values against MRSA USA300 of ≤2 μg mL^{-1} were selected for further antimicrobial evaluation. The antibacterial activity of the three compounds was investigated against a panel of clinically important staphylococcal strains, including methicillin-sensitive *S. aureus* (MSSA), methicillin-resistant *S. aureus* (MRSA), and vancomycin-resistant *S. aureus* (VRSA). It is worth noting that MRSA USA300 is responsible for most MRSA infections in the United States.[28] Meanwhile, MRSA USA400 is the cause of 98% of MRSA infections in the northern communities in Canada.[29] MRSA USA500 has also been associated with community and

Table 2 Initial antibacterial assessment of the tested compounds, MIC values in μg mL^{-1} against MRSA USA300

Compound number	R	MIC against MRSA USA 300	Compound number	R	MIC against MRSA USA 300
3d		8	**15d**		1
4d		32	**16d**		4
5d	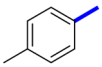	4	**17d**	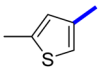	2
6d		8	**18d**	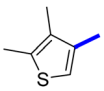	4
7d	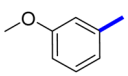	2	**19d**	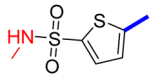	32
8d	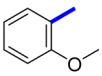	2	**20d**	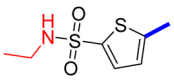	16
9d	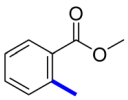	8	**21d**	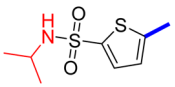	32
10d	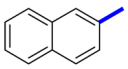	4	**22d**	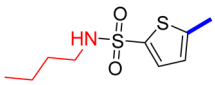	>32
11d	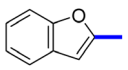	32	**23d**	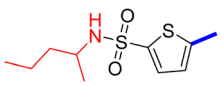	16
12d	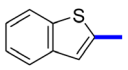	32	**24d**	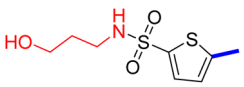	>32
13d		64	**25d**	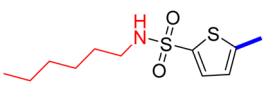	>32
14d		2	**26d**	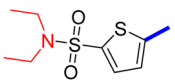	16
Vancomycin		1			

hospital-acquired outbreaks with high morbidity and mortality rates.[29–32]

Our compounds exhibited potent antibacterial activity against the tested MSSA, MRSA, and VRSA strains, inhibiting their growth at concentrations ranging from 0.5 to 4 μg mL^{-1}. Notably, they maintained their potency against linezolid-resistant and vancomycin-resistant staphylococcal strains. Compound **15d** displayed the most potent activity against the tested strains, inhibiting their growth at concentrations ranging from 0.5 to 1 μg mL^{-1} (Table 3). Interestingly, the compounds maintained their potency against linezolid-resistant and vancomycin-resistant staphylococcal strains, suggesting that they do not share the same resistance mechanism with linezolid or vancomycin.

2.2.3. The minimum inhibitory concentrations of compounds 7d, 15d and 17d against other clinically important Gram-positive bacteria. Next, the spectrum of the antibacterial activity of the phenylthiazole compounds was examined against a panel of clinically relevant Gram-positive bacterial pathogens, including *Streptococcus pneumoniae*, vancomycin-resistant *Enterococcus faecium* and *Enterococcus faecalis* (VRE), and *Listeria monocytogenes* and *Clostridioides difficile* (Table 4). Our compounds exhibited potent antibacterial activity against the clinically important drug-resistant Gram-positive pathogens, inhibiting the growth of the tested strains at concentrations of 1 to 4 μg mL^{-1}. Also, they maintained the same activity range against different Gram-positive bacteria.

Table 3 MICs (μg mL^{-1}) of the tested compounds against staphylococcal strains

	Compounds/control antibiotics				
Bacterial isolates	**7d**	**15d**	**17d**	Linezolid	Vancomycin
MSSA ATCC 6538	2	1	4	1	0.5
MSSA NRS 107	4	1	4	0.5	1
MRSA NRS 119	4	1	4	64	2
MRSA USA 400	2	0.5	2	2	1
MRSA USA 500	4	1	4	1	2
MRSA USA 700	2	1	4	1	1
VRSA 9	2	0.5	4	1	>64
VRSA 10	2	1	4	2	64
VRSA 12	4	1	4	1	>64
S. epidermidis NRS 101	2	0.5	2	1	1

Table 4 MICs (μg mL^{-1}) of the three tested compounds against clinically important Gram-positive bacterial pathogens

	Compounds/control antibiotics				
Bacterial isolates	**7d**	**15d**	**17d**	Linezolid	Vancomycin
S. pneumoniae ATCC 51916	4	1	4	1	2
S. pneumoniae ATCC 700677	4	1	4	1	1
E. faecalis ATCC 51299	4	2	4	1	64
E. faecium ATCC 700221	2	1	2	1	>64
L. monocytogenes ATCC 19111	4	1	8	1	1
C. difficile ATCC BAA 1870	4	2	2	NT	1

Among the tested compounds, compound **15d** displayed the most potent activity among the tested compounds with MIC values ranging from 1 μg mL^{-1} to 2 μg mL^{-1}. Compounds **7d** and **17d** also exhibited strong activity, inhibiting the bacterial strains at MICs ranging from 2 to 8 μg mL^{-1}. Importantly, our compounds maintained their potency against vancomycin-resistant enterococcal strains, suggesting that they are not subjected to the same resistance mechanism as vancomycin.

2.2.4. Toxicity profile. The toxicity evaluation is an essential step in the development of new compounds with potential antibacterial activity, as it is important to ensure that these compounds do not cause harm to the host tissues. In this study, compounds **7d**, **15d**, and **17d** were assessed for their toxicity using Caco-2 cells, and were found to have good toxicity profiles. Specifically, at high concentrations, these compounds demonstrated well-tolerated effects on Caco-2 cells. Compound **17d** was found to be highly tolerable to Caco-2 cells at

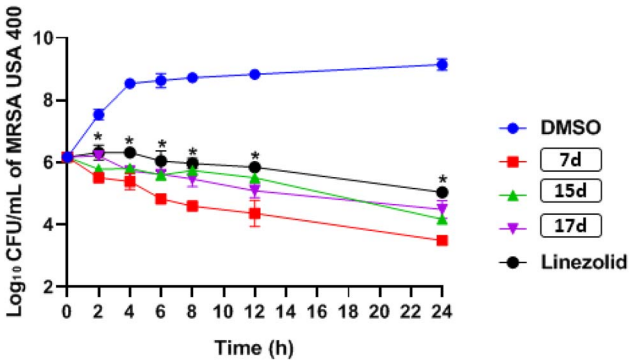

Fig. 3 Killing kinetics of compounds (tested in triplicates at 5 × MIC) against methicillin-resistant *Staphylococcus aureus* NRS123 over a 24 hours incubation period at 37 °C. DMSO (solvent for the compounds) served as a negative control, and linezolid and vancomycin served as control antibiotics. The error bars represent standard deviation values obtained from triplicate samples used for each compound/antibiotic studied. Data were analyzed *via* a two-way ANOVA with post hoc Dunnett's test for multiple comparisons. An asterisk (*) denotes a statistical difference ($p < 0.05$) between the values obtained for each test agent as compared to DMSO.

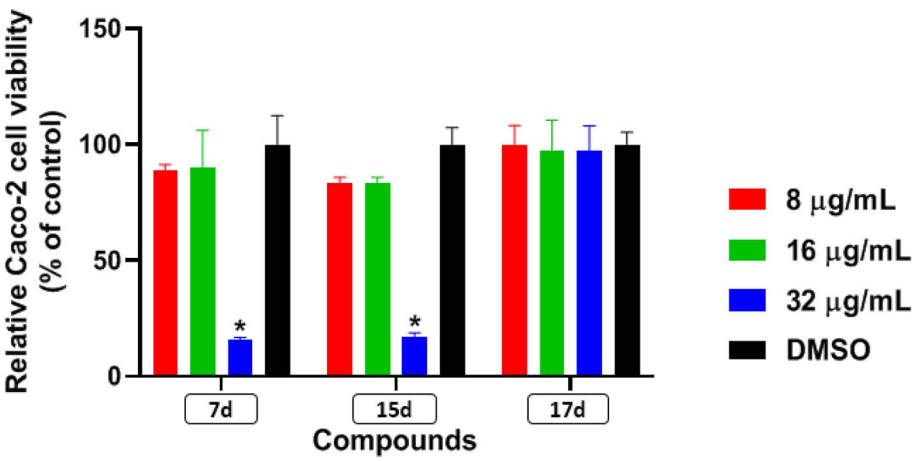

Fig. 2 Analyzing the toxicity of compounds **7d**, **15d** and **17d** (tested in triplicates at 8, 16 and 32 μg mL^{-1}) against human colorectal cells (Caco-2) using the MTS 3-(4,5-dimethylthiazol-2-yl)-5-(3-carboxymethoxyphenyl)-2-(4-sulfophenyl)-2*H*-tetrazolium assay. Results are presented as the percentage of viable cells relative to DMSO (negative control) to determine a baseline measure for the cytotoxic impact of each compound. The absorbance values represent an average of three samples analyzed for each compound. Error bars represent the standard deviation values. Data were analyzed *via* a two-way ANOVA with post hoc Dunnett's test for multiple comparisons. (*) denotes a statistical difference ($p < 0.05$) between values obtained for the compounds and the DMSO.

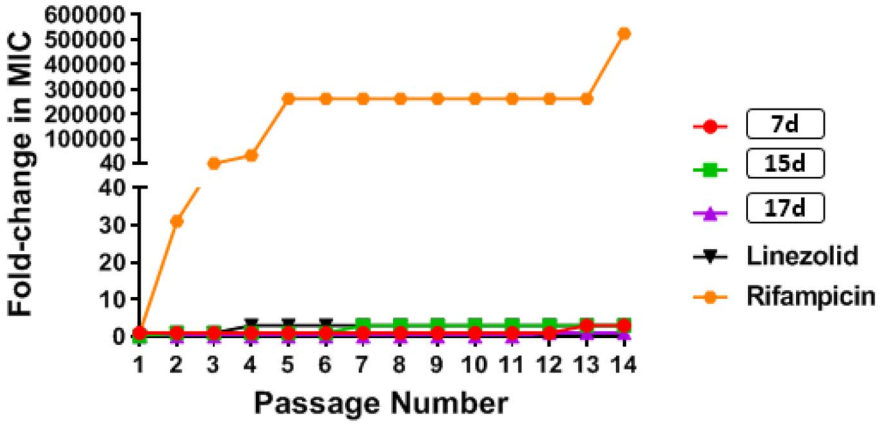

Fig. 4 Multi-step resistance selection of compounds against methicillin-resistant *S. aureus* USA 400. Bacteria were serially passaged over a 14 days period, and the broth microdilution assay was used to determine the minimum inhibitory concentration of each compound against MRSA after each successive passage. A four-fold shift in MIC would be indicative of bacterial resistance to the test agent.

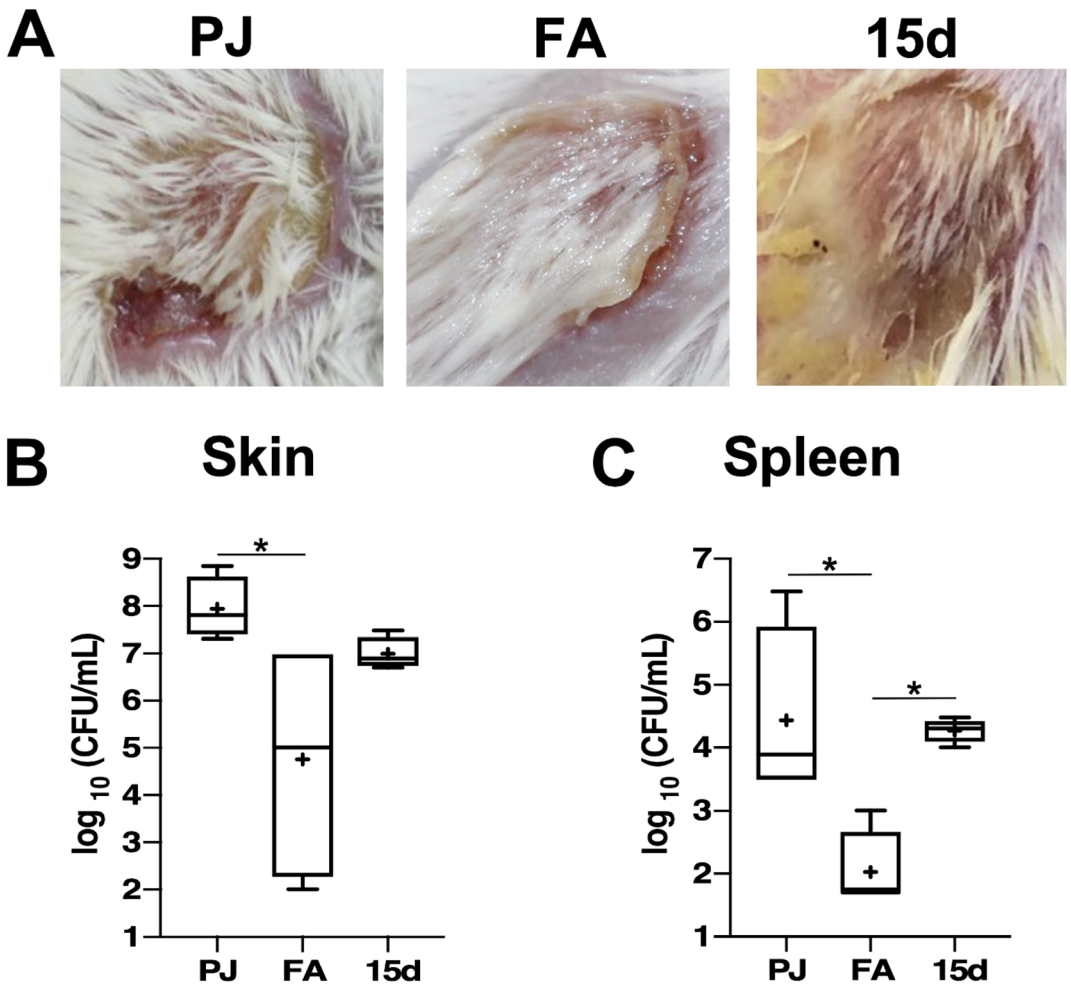

Fig. 5 *In vivo* anti-MRSA activity in a murine model of skin infection. Seventy-two hours post-infection with *S. aureus* USA300, a visible lesion developed at the site of infection. Twice a day topical application of petroleum jelly (PJ), commercial 2% fusidic acid ointment (FA) or 2% **15d** in PJ (**15d**) was carried out for 4 consecutive days. (A) Photographs of representative mice from the three groups on the sacrifice day. Box plots of the bacterial burden recovered from the skin lesions (B) and the spleens (C) of the infected mice of the three groups. In both plots, the whiskers span the difference between the minimum and maximum readings, the horizontal bar represents the median, and the (+) sign represents the mean of the $\log_{10}$CFU mL^{-1}. Statistical analysis was done using the ordinary one-way ANOVA, followed by Tukey's multiple comparisons test. The * indicates a statistical difference ($p \leq 0.05$). The charts were generated using GraphPad Prism (version 9.0).

concentrations of up to 32 μg mL^{-1}, with 100% of the cells remaining viable. Similarly, compounds **7d** and **15d** were found to be highly tolerable to Caco-2 cells at concentrations of up to 16 μg mL^{-1}, with 100% of the cells remaining viable. These results are shown in Fig. 2.

2.2.5. Time kill kinetics assay. To investigate the mode of killing of the phenylthiazole compounds, we conducted a time-kill kinetics assay against MRSA NRS123. Similar to linezolid, compounds **7d**, **15d**, and **17d** exhibited bacteriostatic activity against MRSA, inhibiting bacterial reproduction. However, they also resulted in a significant reduction in bacterial count compared to the negative control (DMSO). Compound **7d** resulted in a 2.7 $\log_{10}$ – reduction after 24 hours, while compounds **15d** and **17d** generated 2.0 and 1.7 $\log_{10}$ – reduction in bacterial CFU, respectively. In contrast, linezolid resulted in only a 1.1 $\log_{10}$ -reduction in bacterial burden after 24 hours (see Fig. 3).

2.2.6. Multi-step resistance study against MRSA. To test the potential for MRSA to develop resistance against phenylthiazole compounds, a multi-step resistance test was conducted. The MIC values for compound **17d** increased by one-fold only, and remained stable thereafter. The MIC values for compounds **7d** and **15d** increased by two-fold, while the linezolid MICs increased by 2-fold after 14 passages. In contrast, MRSA rapidly developed resistance to the antibiotic rifampicin, with the MIC of the antibiotic increasing by 31-fold after just one passage. It continued to increase rapidly, with a more than 500 000-fold increase in MIC by the end of the experiment. These results indicate that MRSA was unable to develop rapid resistance to any of the tested phenylthiazole compounds, but could rapidly develop resistance to rifampicin (Fig. 4).

2.2.7. *In vivo* anti-MRSA activity in a murine model of skin infection. This section presents the results of an *in vivo* experiment to assess the efficacy of compound **15d** in controlling a *S. aureus* skin infection. The experiment included a positive control group treated with fusidic acid (FA), given its well-known anti-staphylococcal effect, and a vehicle control group treated with petroleum jelly (PJ). Mice were infected subcutaneously with MRSA USA300, and skin lesions were observed 72 hours post-infection. The group treated with PJ alone experienced extensive skin damage and open lesions, which continued to progress until the end of the experiment. In contrast, mice treated with either compound **15d** or FA showed considerable healing, and less ulceration and scab formation (Fig. 5A).

Bacterial burdens in the skin lesions were estimated, and it was observed that compound **15d** resulted in a decrease in the MRSA burden in the mice skin lesions by almost one $\log_{10}$ cycle, which was not significant compared to the FA treatment that generated around three $\log_{10}$ reduction as compared to the vehicle-treated mice (Fig. 5B). However, compound **15d** demonstrated weaker activity than FA in controlling the systemic dissemination of *S. aureus*, as evidenced by the low reduction in the bacterial burden detected in the spleens of infected mice compared to the vehicle-treated group (Fig. 5C). These results suggest that while compound **15d** shows promising potential in controlling *S. aureus* skin infection, its efficacy in controlling systemic dissemination is weaker than that of FA.

3. Conclusion

The present study aimed to enhance the antibacterial activity of phenylthiazoles against multidrug-resistant *Staphylococci* by exploring the lipophilic part of the compounds *via* Suzuki coupling reaction. First, twenty-three compounds were synthesized, and their efficacy was evaluated against a range of clinical isolates, including MRSA USA400, MRSA NRS119, and vancomycin-resistant isolates VRSA 9/10/12. Compound **15d** was found to be particularly potent, exhibiting an inhibitory concentration of 0.5 μg mL^{-1} against MRSA USA400, which is one-fold more potent than vancomycin. Additionally, compound **15d** maintained its efficacy against ten clinical isolates, including MRSA NRS119 and three VRSA strains. *In vivo* experiments on skin-infected mice showed that compound **15d** was able to reduce the bacterial burden of MRSA USA300. These results provide evidence that exploring the lipophilic part of phenylthiazoles is promising, and can lead to the development of more potent antibiotics against multidrug-resistant *Staphylococci*.

4. Experimental

4.1. Chemistry

General: ^{1}H NMR spectra were run at 400 MHz and ^{13}C NMR spectra were determined at 100 MHz in dimethyl sulfoxide (DMSO-d_6) on a Bruker VX-400 NMR spectrometer. Chemical shifts are given in parts per million (ppm) on the delta (δ) scale. Chemical shifts were calibrated relative to those of the solvents. Flash chromatography was performed on 230–400 mesh silica. The progress of reactions was monitored with Merck silica gel IB2-F plates (0.25 mm thickness). The infrared spectra were recorded in potassium bromide disks on pye Unicam SP 3300 and Shimadzu FT IR 8101 PC infrared spectrophotometer. Mass spectra were recorded at 70 eV. High-resolution mass spectra for all ionization techniques were obtained from a FinniganMAT XL95. Melting points were determined using capillary tubes with a Stuart SMP30 apparatus and are uncorrected. All yields reported refer to isolated yields.

4.1.1. Preparation of sulfonamide intermediates (19–25). To a solution of 5-bromothiophene-2-sulfonyl chloride (0.13 g, 0.5 mmol) in dichloromethane (0.67 M), an appropriate amine (0.75 mmol) and triethylamine (0.1 g, 1 mmol) were added. The reaction mixture was stirred at room temperature for 1 h, then washed with water, and the aqueous layer was extracted with dichloromethane. The combined organic layer was dried over ($MgSO_4$), filtered and evaporated under reduced pressure. The residue was purified by flash chromatography (hexane : ethyl acetate = 4 : 1) to afford compounds **19–25** as white solids as reported.[33–35]

4.1.2. Preparation of compounds (3c–25c)

4.1.2.1 General procedure. A. Direct method: To a dioxan : water (9 : 1 mL) mixture in a 75 mL sealed tube, compound **2b**

(350 mg, 1.02 mmol), palladium diacetate (24 mg, 10% mol), 2-dicyclohexylphosphino-2′,4′,6′-triiso-propylbiphenyl (X-phos) (146 mg, 0.3 mmol) and Cesium carbonate (833 mg, 2.56 mmol) were dissolved. After the reaction mixture was purged with dry nitrogen gas for 10 min, appropriate bronic acid derivatives (1.61 mmol) were added. The sealed tube was then placed in an oil bath and stirred at 100 °C for 24 h. After cooling to room temperature, the reaction mixture was passed through Celite, followed by ethyl acetate (2 × 50 mL), and dried over anhydrous magnesium sulphate. The organic materials were then concentrated under reduced pressure. The crude materials were purified *via* silica gel flash column chromatography using hexane–ethyl acetate (7 : 3).

B. In situ: In a 75 mL sealed tube with 15 mL EtOH, compound **2a** (350 mg, 1.39 mmol, 1 eq.), tetrahydroxydiboron (373.94 mg, 4.17 mmol, 3 eq.), XPhos-PdG2 (11 mg, 14 μmol, 0.01 eq.), XPhos (13.23 mg, 28 μmol, 0.02 eq.), and NaOAc (342 mg, 4.17 mmol, 3 eq.) were added respectively under N_2 flushing. The reaction mixture was then heated to 80 °C until the solution changed into a red color, and a precipitation was formed, indicating that the boronic acid derivative was formed and confirmed by TLC. Then, a solution of K_2CO_3 (577 mg, 4.17 mmol, 3 eq.) in 5 mL distilled water was added to the reaction mixture, followed by the addition of the second halide (2.8 mmol, 2 eq.). The reaction mixture was further heated to 80 °C for 15 h. After cooling to room temperature, the reaction mixture was passed through Celite, followed by ethyl acetate (2 × 50 mL) and dried over anhydrous magnesium sulphate. The organic materials were then concentrated under reduced pressure. The crude materials were purified *via* silica gel flash column chromatography using hexane–ethyl acetate (7 : 3).

*1-(2-(4-Isobutylphenyl)-4-methylthiazol-5-yl)ethan-1-one (**3c**)*: Following the general procedure (method A), compound **3c** was obtained as a light-brown oil (240 mg, 86%). ^{1}H NMR (DMSO-d_6) δ: 8.01 (d, J = 8.2 Hz, 2H), 7.28 (d, J = 8.2 Hz, 2H), 2.71 (s, 3H), 2.62 (s, 3H), 2.52 (d, J = 7.2 Hz, 2H), 1.93–1.83 (m, 1H), 0.90 (d, J = 8.2 Hz, 6H); ^{13}C NMR (DMSO-d_6); δ 200.6, 148.5, 142.3, 137.0, 135.2, 129.7, 126.6, 117.2, 44.8, 30.1, 25.2, 22.6, 17.5; MS (*m*/*z*); 273.

*1-(2-(4-Cyclopropylphenyl)-4-methylthiazol-5-yl)ethan-1-one (**4c**)*: Following the general procedure (method A), compound **4c** was obtained as a light-brown oil (226 mg, 86%). ^{1}H NMR (DMSO-d_6) δ: 7.98 (d, J = 8.2 Hz, 2H), 7.18 (d, J = 8.2 Hz, 2H), 2.64 (s, 3H), 2.23 (s, 3H), 1.99–194 (m, 1H), 1.01–0.97 (m, 2H), 0.75–0.72 (m, 2H); ^{13}C NMR (DMSO-d_6); δ 196.0, 153.4, 146.0, 137.0, 136.1, 135.1, 126.03, 117.0, 25.2, 17.5, 15.4, 10.1; MS (*m*/*z*); 257.

*1-(4-Methyl-2-(4′-methyl-[1,1′-biphenyl]-4-yl)-thiazol-5-yl)ethan-1-one (**5c**)*: Following the general procedure (method A), compound **5c** was obtained as a yellow oil (293 mg, 93%). ^{1}H NMR (DMSO-d_6) δ: 7.97 (d, J = 8.4 Hz, 2H), 7.77 (d, J = 8.4 Hz, 2H), 7.64 (d, J = 8.4 Hz, 2H), 7.31 (d, J = 8.2 Hz, 2H), 2.61 (s, 3H), 2.36 (s, 3H), 2.33 (s, 3H); MS (*m*/*z*); 307.

*1-(4-Methyl-2-(3′-methyl-[1,1′-biphenyl]-4-yl)thiazol-5-yl)ethan-1-one (**6c**)*: Following the general procedure (method A), compound **6c** was obtained as a light brown oil (246 mg, 78%). ^{1}H NMR (DMSO-d_6) δ: 8.20 (d, J = 8.4 Hz, 2H), 7.78 (d, J = 8.4 Hz, 2H), 7.56 (s, 1H), 7.53 (d, J = 8.2 Hz, 1H), 7.40 (t, J = 8.2 Hz, 1H), 7.22 (d, J = 8.2 Hz, 1H), 2.67 (s, 3H), 2.40 (s, 3H), 2.26 (s, 3H); MS (*m*/*z*); 307.

*1-(2-(3′-Methoxy-[1,1′-biphenyl]-4-yl)-4-methylthiazol-5-yl) ethan-1-one (**7c**)*: Following the general procedure (method B), compound **7c** was obtained as a yellow oil (193 mg, 43%). ^{1}H NMR (DMSO-d_6) δ: 8.08 (d, J = 8 Hz, 2H), 7.85 (d, J = 8 Hz, 2H), 7.74 (t, J = 8 Hz, 1H), 7.32 (d, J = 8 Hz, 1H), 7.27 (s, 1H), 7.01 (d, J = 8 Hz, 1H), 3.85 (s, 3H), 2.73 (s, 3H), 2.58 (s, 3H); ^{13}C NMR (DMSO-d_6); δ: 192.1, 168.5, 160.3, 158.7, 143.2, 140.8, 132.6, 131.7, 130.6, 128.1, 127.5, 119.5, 114.3, 112.6, 55.6, 30.6, 18.6; MS (*m*/*z*); 323.

*1-(2-(2′-Methoxy-[1,1′-biphenyl]-4-yl)-4-methylthiazol-5-yl) ethan-1-one (**8c**)*: Following the general procedure (method B), compound **8c** was obtained as a buff oil (188 mg, 42%). ^{1}H NMR (DMSO-d_6) δ: 8.03 (d, J = 8 Hz, 2H), 7.65 (d, J = 8 Hz, 2H), 7.41–7.36 (m, 2H), 7.16 (t, J = 8 Hz, 1H), 7.08 (t, J = 8 Hz, 1H), 3.79 (s, 3H), 2.72 (s, 3H), 2.57 (s, 3H); ^{13}C NMR (DMSO-d_6); δ: 191.8, 168.8, 158.6, 156.6, 141.7, 132.5, 131.0, 130.7, 130.6, 130.0, 129.0, 126.7, 121.3, 112.3, 55.0, 30.8, 18.6; MS (*m*/*z*); 323.

*Methyl 4′-(5-acetyl-4-methylthiazol-2-yl)-[1,1′-biphenyl]-2-carboxylate (**9c**)*: Following the general procedure (method B), compound **9c** was obtained as a yellow oil (293 mg, 60%). ^{1}H NMR (DMSO-d_6) δ: 8.05 (d, J = 8 Hz, 2H), 7.82 (d, J = 8 Hz, 1H), 7.69 (t, J = 8 Hz, 1H), 7.56 (t, J = 8 Hz, 1H), 7.50 (d, J = 8 Hz, 1H), 7.45 (d, J = 8 Hz, 2H), 3.64 (s, 3H), 2.73 (s, 3H), 2.58 (s, 3H); ^{13}C NMR (DMSO-d_6); δ: 191.1, 168.6, 158.7, 144.0, 140.7, 132.6, 131.5, 130.9, 130.0, 129.6, 128.5, 126.9, 128.5, 126.9, 52.5, 30.9, 18.6; MS (*m*/*z*); 351.

*1-(4-Methyl-2-(4-(naphthalen-2-yl)phenyl)-thiazol-5-yl)ethan-1-one (**10c**)*: Following the general procedure (method A), compound **10c** was obtained as a yellow oil (302 mg, 86%). ^{1}H NMR (DMSO-d_6) δ: 8.30 (s, 1H), 8.25 (d, J = 8.4 Hz, 2H), 7.95 (d, J = 8.4 Hz, 2H), 7.90 (s, 1H), 7.80 (t, J = 8.4 Hz, 1H), 7.58 (t, J = 8.4 Hz, 1H), 7.54 (d, J = 8.4 Hz, 2H), 7.40 (d, J = 8.2 Hz, 1H), 2.69 (s, 3H), 2.26 (s, 3H); MS (*m*/*z*); 343.

*1-(2-(4-Benzofuran-2-yl)phenyl)-4-methylthiazol-5-yl)ethan-1-one (**11c**)*: Following the general procedure (method A), compound **14c** was obtained as a yellow oil (280 mg, 82%). ^{1}H NMR (DMSO-d_6) δ: 8.26 (d, J = 8.4 Hz, 2H), 8.04 (d, J = 8.4 Hz, 2H), 7.80 (d, J = 8.4 Hz, 1H), 7.70 (d, J = 8.4 Hz, 1H), 7.68 (s, 1H), 7.57 (t, J = 8.4 Hz, 1H), 7.35 (t, J = 8.2 Hz, 1H), 2.67 (s, 3H), 2.25 (s, 3H); MS (*m*/*z*); 333.

*1-(2-(4-Benzo[b]thiophen-2-yl)phenyl)-4-methylthiazol-5-yl) ethan-1-one (**12c**)*: Following the general procedure (method A), compound **12c** was obtained as a yellow oil (290 mg, 81%). ^{1}H NMR (DMSO-d_6) δ: 8.23 (d, J = 8.4 Hz, 2H), 7.99 (d, J = 8.4 Hz, 2H), 7.89 (d, J = 8.4 Hz, 1H), 7.86 (s, 1H), 7.82 (t, J = 8.4 Hz, 1H), 7.78 (d, J = 8.4 Hz, 1H), 7.57 (t, J = 8.2 Hz, 1H), 2.67 (s, 3H), 2.25 (s, 3H); MS (*m*/*z*); 349.

*1-(2-(4-Furan-2-yl)phenyl)-5-methylthiazol-5-yl)ethan-1-one (**13c**)*: Following the general procedure (method A), compound **13c** was obtained as a yellow oil (250 mg, 86%). ^{1}H NMR (DMSO-d_6) δ: 8.01 (d, J = 8.2 Hz, 2H), 7.80 (d, J = 8.2 Hz, 2H), 7.66 (d, J = 8.4 Hz, 2H), 7.20 (t, J = 8.4 Hz, 1H), 2.71 (s, 3H), 2.56 (s, 3H); ^{13}C NMR (DMSO-d_6); δ 191.0, 168.3, 158.7, 142.9, 136.8, 132.4, 131.3, 129.3, 127.7, 127.5, 126.4, 125.4, 30.8, 18.6; MS (*m*/*z*); 283.

*1-(2-(4-Furan-3-yl)phenyl)-5-methylthiazol-5-yl)ethan-1-one (**14c**)*: Following the general procedure (method A), compound **14c** was obtained as a pale-yellow oil (244 mg, 84%). ^{1}H NMR (DMSO-d_6) δ: 8.29 (s, 1H), 7.91 (d, J = 8.2 Hz, 2H), 7.78 (d, J = 8.2 Hz, 1H), 7.73 (d, J = 8.4 Hz, 2H), 7.03 (d, J = 6.4 Hz, 1H), 2.59 (s, 3H), 2.32 (s, 3H); ^{13}C NMR (DMSO-d_6); δ 191.0, 168.6, 158.7, 140.7, 138.2, 132.3, 131.5, 129.8, 127.9, 127.5, 125.5, 122.9, 30.8, 18.6; MS (m/z); 283.

*1-(4-Methyl-2-(4-(thiophen-2-yl)phenyl)thiazol-5-yl)ethan-1-one (**15c**)*: Following the general procedure (method B), compound **15c** was obtained as a yellow oil (263 mg, 63%). ^{1}H NMR (DMSO-d_6) δ: 8.01 (d, J = 8 Hz, 2H), 7.70 (d, J = 8 Hz, 2H), 7.66–7.64 (m, 2H), 7.20–7.18 (m, 1H), 2.70 (s, 3H), 2.56 (s, 3H); ^{13}C NMR (DMSO-d_6); δ 191.0, 168.3, 158.7, 142.5, 136.8, 132.4, 131.3, 129.3, 127.7, 127.5, 126.4, 125.4, 30.8, 18.6; MS (m/z); 299.

*1-(4-Methyl-2-(4-(thiophen-3-yl)phenyl)thiazol-5-yl)ethan-1-one (**16c**)*: Following the general procedure (method B), compound **16c** was obtained as a yellow oil (210 mg, 50%). ^{1}H NMR (DMSO-d_6) δ: 8.02 (d, J = 8 Hz, 2H), 7.98 (s, 1H), 7.86 (d, J = 8 Hz, 2H), 7.68 (d, J = 8 Hz, 1H), 7.63 (d, J = 8 Hz, 1H), 2.7 (s, 3H), 2.55 (s, 3H); ^{13}C NMR (DMSO-d_6); δ 191.0, 168.4, 158.5, 140.7, 136.2, 132.5, 132.3, 131.1, 127.9, 127.2, 126.5, 122.9, 30.8, 18.6; MS (m/z); 299.

*1-(4-Methyl-2-(4-(5-methylthiophen-3-yl)phenyl)thiazol-5-yl) ethan-1-one (**17c**)*: Following the general procedure (method B), compound **17c** was obtained as a brown oil (180 mg, 41%). ^{1}H NMR (DMSO-d_6) δ: 8.01 (d, J = 8 Hz, 2H), 7.82 (d, J = 8 Hz, 2H), 7.77 (s, 1H), 7.33 (s, 1H), 2.71 (s, 3H), 2.57 (s, 3H), 2.39 (s, 3H); ^{13}C NMR (DMSO-d_6); δ 191.0, 168.6, 158.7, 141.0, 140.3, 138.4, 132.3, 130.9, 127.5, 126.9, 124.8, 120.8, 30.9, 18.6, 15.5; MS (m/z); 313.

*1-(2-(4-(4,5-Dimethylthiophen-3-yl)phenyl)-4-methylthiazol-5-yl)ethan-1-one (**18c**)*: Following the general procedure (method B), compound **18c** was obtained as a yellow oil (305 mg, 67%). ^{1}H NMR (DMSO-d_6) δ: 8.03 (d, J = 8 Hz, 2H), 7.52 (d, J = 8 Hz, 2H), 7.32 (s, 1H), 2.72 (s, 3H), 2.57 (s, 3H), 2.38 (s, 3H), 2.12 (s, 3H); ^{13}C NMR (DMSO-d_6); δ 191.0, 168.4, 158.5, 142.3, 140.5, 134.3, 132.5, 131.4, 131.0, 129.5, 127.0, 120.4, 30.8, 18.5, 13.9, 13.4; MS (m/z); 327.

*5-[4-(5-Acetyl-4-methylthiazol-2-yl)phenyl]-N-methylthiophene-2-sulfonamide (**19c**)*: Following the general procedure (method B), compound **19c** was obtained as a yellow oil (130 mg, 23%); ^{1}H NMR (DMSO-d_6) δ: 8.06 (d, J = 8.4 Hz, 2H), 7.88 (d, J = 8.4 Hz, 2H), 7.79 (brs, 1H), 7.72 (d, J = 4 Hz, 1H), 7.62 (d, J = 4 Hz, 1H), 2.71 (s, 3H), 2.57 (s, 3H), 2.56 (s, 3H); ^{13}C NMR (DMSO-d_6) δ: 191.1, 167.9, 158.7, 148.0, 140.1, 135.2, 133.2, 132.9, 132.7, 127.8, 127.1, 125.6, 30.9, 29.3, 18.6; MS (m/z) 392.

*5-[4-(5-Acetyl-4-methylthiazol-2-yl)phenyl]-N-ethylthiophene-2-sulfonamide (**20c**)*: Following the general procedure (method B), compound **20c** was obtained as a yellow oil (150 mg, 27%); ^{1}H NMR (DMSO-d_6) δ: 8.06 (d, J = 8.4 Hz, 2H), 7.90 (brs, 1H), 7.88 (d, J = 8.4 Hz, 2H), 7.71 (d, J = 4 Hz, 1H), 7.61 (d, J = 4 Hz, 1H), 2.94 (m, 2H), 2.73 (s, 3H), 2.58 (s, 3H), 1.07 (t, J = 7.2 Hz, 3H); ^{13}C NMR (DMSO-d_6) δ: 191.1, 167.9, 158.7, 147.8, 141.5, 135.2, 132.96, 132.90, 132.6, 127.8, 127.1, 125.6, 38.3, 30.9, 18.6, 15.1; MS (m/z) 406.

*5-[4-(5-Acetyl-4-methylthiazol-2-yl)phenyl]-N-isopropylthiophene-2-sulfonamide (**21c**)*: Following the general procedure (method B), compound **21c** was obtained as a yellow oil (160 mg, 28%); ^{1}H NMR (DMSO-d_6) δ: 8.07 (d, J = 8.4 Hz, 2H), 7.95 (brs, 1H), 7.89 (d, J = 8.4 Hz, 2H), 7.70 (d, J = 4 Hz, 1H), 7.61 (d, J = 4 Hz, 1H), 3.46 (m, 1H), 2.72 (s, 3H), 2.58 (s, 3H), 1.07 (m, 6H); ^{13}C NMR (DMSO-d_6) δ: 191.1, 167.9, 158.7, 147.6, 142.9, 135.3, 132.89, 132.80, 132.6, 127.8, 127.0, 125.5, 46.2, 30.9, 23.6, 19.0; MS (m/z) 421.

*5-(4-(5-Acetyl-4-methylthiazol-2-yl)phenyl)-N-butylthiophene-2-sulfonamide (**22c**)*: Following the general procedure (method B), compound **22c** was obtained as a yellow oil (175 g, 30%); ^{1}H NMR (DMSO-d_6) δ: 8.07 (d, J = 8.4 Hz, 2H), 7.92 (brs, 1H), 7.88 (d, J = 8.4 Hz, 2H), 7.71 (d, J = 4 Hz, 1H), 7.61 (d, J = 4 Hz, 1H), 2.92 (m, 2H), 2.73 (s, 3H), 2.58 (s, 3H), 1.43 (m, 2H), 1.31 (m, 2H), 0.84 (t, J = 7.2 Hz, 3H); ^{13}C NMR (DMSO-d_6) δ: 191.1, 167.9, 158.7, 147.8, 141.5, 135.2, 132.96, 132.90, 132.6, 127.8, 127.1, 125.6, 42.9, 31.4, 30.9, 19.7, 18.6, 13.9; MS (m/z) 434.

*5-[4-(5-Acetyl-4-methylthiazol-2-yl)phenyl]-N-(pentan-2-yl) thiophene-2-sulfonamide (**23c**)*: Following the general procedure (method B), compound **23c** was obtained as a yellow oil (134 mg, 22%); ^{1}H NMR (DMSO-d_6) δ: 8.08 (d, J = 8.4 Hz, 2H), 7.89 (brs, 1H), 7.87 (d, J = 8.4 Hz, 2H), 7.70 (d, J = 4 Hz, 1H), 7.61 (d, J = 4 Hz, 1H), 3.30–3.20 (m, 1H), 2.72 (s, 3H), 2.58 (s, 3H), 1.33–1.21 (m, 4H), 0.99–0.97 (m, 3H), 0.79–0.77 (m, 3H); ^{13}C NMR (DMSO-d_6) δ: 191.3, 167.9, 158.7, 147.5, 143.2, 135.3, 132.9, 132.7, 132.6, 127.9, 127.0, 125.5, 49.8, 30.9, 21.5, 18.8, 18.6, 14.1; MS (m/z) 448.6.

*5-[4-(5-Acetyl-4-methylthiazol-2-yl)phenyl]-N-hexylthiophene-2-sulfonamide (**24c**)*: Following the general procedure (method B), compound **24c** was obtained as a yellow oil (144 mg, 22%); ^{1}H NMR (DMSO-d_6) δ: 8.06 (d, J = 8.4 Hz, 2H), 7.92 (brs, 1H), 7.88 (d, J = 8.4 Hz, 2H), 7.70 (d, J = 4 Hz, 1H), 7.60 (d, J = 4 Hz, 1H), 2.90 (q, J = 6.8 Hz, 2H), 2.72 (s, 3H), 2.58 (s, 3H), 1.45–1.38 (m, 2H), 1.28–1.16 (m, 6H), 0.83–0.80 (t, J = 6.4 Hz, 3H); ^{13}C NMR (DMSO-d_6) δ: 191.0, 167.9, 158.7, 147.8, 141.6, 135.2, 132.9, 132.6, 132.2, 127.8, 127.0, 125.5, 43.2, 31.2, 30.9, 29.2, 26.1, 22.4, 18.6, 14.3; MS (m/z) 462.11.

*5-[4-(5-Acetyl-4-methylthiazol-2-yl)phenyl]-N,N-diethylthiophene-2-sulfonamide (**25c**)*: Following the general procedure (method B), compound **25c** was obtained as a light yellow oil (280 mg, 46%); ^{1}H NMR (DMSO-d_6) δ: 8.06 (d, J = 8.4 Hz, 2H), 7.9 (d, J = 8.4 Hz, 2H), 7.74 (d, J = 4 Hz, 1H), 7.69 (d, J = 4 Hz, 1H), 3.25 (q, J = 7.2 Hz, 4H), 2.72 (s, 3H), 2.58 (s, 3H), 1.14 (t, J = 7.2 Hz, 6H); ^{13}C NMR (DMSO-d_6) δ: 192.2, 167.9, 158.7, 148.2, 139.6, 135.1, 133.3, 132.9, 132.7, 127.8, 127.1, 125.8, 42.9, 30.9, 18.6, 14.6; MS (m/z) 434.

4.1.3. Preparation of compounds 3–25d

4.1.3.1 General procedure. Acetyl derivatives **3–25c** (0.375 mmol) was dissolved in absolute ethanol (15 mL), then concentrated hydrochloric acid (0.5 mL) and aminoguanidine hydrochloride (0.75 mmol) were added. The reaction mixture was heated at reflux for 4 h. The solvent was concentrated under reduced pressure, then poured into crushed ice and neutralized with sodium carbonate to pH 7–8. The formed precipitated solid was collected by filtration, and washed with a copious

amount of water. Crystallization from dichloromethane afforded the desired products.

*2-(1-(2-(4-Isobutylphenyl)-4-methylthiazol-5-yl)ethylidene) hydrazine-1-carboximidamide (**3d**)*: Light-brown solid (90 mg, 73%); mp 117–119 °C; ^{1}H NMR (DMSO-d_6) δ: 8.01 (d, J = 8.4 Hz, 2H), 7.28 (d, J = 8.4 Hz, 2H), 5.70 (brs, 2H), 5.50 (brs, 2H), 2.63 (s, 3H), 2.52 (d, J = 8.4 Hz, 2H), 2.23 (s, 3H), 1.90–1.85 (m, 1H), 0.91 (d, J = 8.4 Hz, 6H); ^{13}C NMR (DMSO-d_6); δ 160.2, 155.4, 153.4, 148.5, 137.0, 135.2, 129.7, 126.6, 117.2, 44.8, 30.1, 25.28, 22.6, 17.5; HPLC purity 95.1% (acetonitrile-3% TEA, 1 : 4).

*2-(1-(2-(4-Cyclopropylphenyl)-4-methylthiazol-5-yl)ethylidene) hydrazine-1-carboximidamide (**4d**)*: Light-brown solid (87 mg, 74%); mp 121–123 °C; ^{1}H NMR (DMSO-d_6) δ: 7.98 (d, J = 8.4 Hz, 2H), 7.18 (d, J = 8.4 Hz, 2H), 5.71 (brs, 2H), 5.50 (brs, 2H), 2.62 (s, 3H), 2.23 (s, 3H), 1.99–1.94 (m, 1H), 1.01–0.97 (t, J = 8.4 Hz, 2H), 0.74–0.72 (t, J = 8.4 Hz, 2H); ^{13}C NMR (DMSO-d_6); δ 160.2, 155.4, 153.4, 148.6, 145.0, 137.0, 136.1, 126.7, 126.0, 25.2, 17.5, 15.4, 10.1; HPLC purity 99% (acetonitrile-3% TEA, 1 : 4).

*2-(1-(4-Methyl-2-(4′-methyl-[1,1′-biphenyl]-4-yl)thiazol-5-yl) ethylidene)hydrazine-1-carboximidamide (**5d**)*: Beige solid (90 mg, 76%); mp 133–135 °C; ^{1}H NMR (DMSO-d_6) δ: 7.97 (d, J = 8.4 Hz, 2H), 7.77 (d, J = 8.4 Hz, 2H), 7.64 (d, J = 8.4 Hz, 2H), 7.31 (d, J = 8.2 Hz, 2H), 5.78 (brs, 2H), 5.71 (brs, 2H), 2.61 (s, 3H), 2.36 (s, 3H), 2.33 (s, 3H); ^{13}C NMR (DMSO-d_6); δ 160.3, 155.6, 152.9, 148.5, 140.7, 137.7, 137.1, 137.0, 135.4, 130.0, 127.3, 126.8, 117.4, 25.3, 21.1, 17.5; HPLC purity 100% (acetonitrile-3% TEA, 1 : 4).

*2-(1-(4-Methyl-2-(3′-methyl-[1,1′-biphenyl]-4-yl)thiazol-5-yl) ethylidene)hydrazine-1-carboximidamide (**6d**)*: Beige solid (97 mg, 71%); mp 137–139 °C; ^{1}H NMR (DMSO-d_6) δ: 8.20 (d, J = 8.4 Hz, 2H), 7.78 (d, J = 8.4 Hz, 2H), 7.56 (s, 1H), 7.53 (d, J = 8.2 Hz, 1H), 7.40 (t, J = 8.2 Hz, 1H), 7.22 (d, J = 8.2 Hz, 1H), 5.82 (brs, 2H), 5.71 (brs, 2H), 2.67 (s, 3H), 2.51 (s, 3H), 2.26 (s, 3H); ^{13}C NMR (DMSO-d_6); δ 160.1, 155.6, 153.0, 148.7, 140.9, 140.0, 138.1, 137.9, 137.1, 135.4, 129.3, 128.7, 127.7, 124.2, 117.4, 25.3, 21.6, 17.5; HPLC purity 99.5% (acetonitrile-3% TEA, 1 : 4).

*2-(1-(2-(3′-Methoxy-[1,1′-biphenyl]-4-yl)-4-methylthiazol-5-yl) ethylidene)hydrazine-1-carboximidamide (**7d**)*: Yellow solid (80 mg, 68%) mp = 125–127 °C; ^{1}H NMR (DMSO-d_6) δ: 7.98 (d, J = 8 Hz, 2H), 7.80 (d, J = 8 Hz, 2H), 7.41 (t, J = 8 Hz, 1H), 7.31 (d, J = 8 Hz, 1H), 7.26 (s, 1H), 6.99 (d, J = 8 Hz, 1H), 5.78 (brs, 2H), 5.67 (brs, 2H), 3.84 (s, 3H), 2.61 (s, 3H), 2.33 (s, 3H); ^{13}C NMR (DMSO-d_6) δ: 162.7, 160.2, 160.1, 140.4, 143.1, 141.5, 141.1, 135.9, 132.8, 130.5, 127.8, 126.6, 119.4, 114.0, 112.5, 55.6, 18.7, 16.5; MS (m/z) 379; HPLC purity 93% (acetonitrile-3% TEA, 1 : 4).

*2-(1-(2-(2′-Methoxy-[1,1′-biphenyl]-4-yl)-4-methylthiazol-5-yl) ethylidene)hydrazine-1-carboximidamide (**8d**)*: Yellow solid (77 mg, 65%) mp = 130–132 °C; ^{1}H NMR (DMSO-d_6) δ: 7.94 (d, J = 8 Hz, 2H), 7.60 (d, J = 8 Hz, 2H), 7.40–7.38 (m, 2H), 7.15 (d, J = 8 Hz, 1H), 7.08 (t, J = 8 Hz, 1H), 5.98 (brs, 4H), 3.79 (s, 3H), 2.61 (s, 3H), 2.33 (s, 3H); ^{13}C NMR (DMSO-d_6) δ: 162.7, 159.7, 156.6, 148.8, 143.6, 140.1, 135.2, 132.1, 130.6, 130.4, 129.8, 129.3, 125.8, 121.3, 112.3, 56.0, 18.6, 16.7; MS (m/z) 379; HPLC purity 90.9% (acetonitrile-3% TEA, 1 : 4).

*Methyl-4′-(5-(1-(2-carbamimidoylhydrazono)ethyl)-4-methyl-thiazol-2-yl)-[1,1′-biphenyl]-2-carboxylate (**9d**)*: Yellow solid (75 mg, 64%) mp = 136 °C; ^{1}H NMR (DMSO-d_6) δ: 7.96 (d, J = 8 Hz, 2H), 7.80 (d, J = 8 Hz, 1H), 7.68 (t, J = 8 Hz, 1H), 7.54–7.51 (m, 2H), 7.41 (d, J = 8 Hz, 2H), 6.22 (brs, 4H), 3.63 (s, 3H), 2.61 (s, 3H), 2.35 (s, 3H); ^{13}C NMR (DMSO-d_6) δ: 173.1, 168.8, 162.6, 159.5, 149.2, 143.8, 142.4, 140.9, 132.5, 132.1, 131.1, 130.8, 129.9, 129.4, 126.0, 52.4, 18.6, 16.9; MS (m/z) 407; HPLC purity 95.7% (acetonitrile-3% TEA, 1 : 4).

*2-(1-(4-Methyl-2-(4-(naphthalen-2-yl)phenyl)thiazol-5-yl) ethylidene)hydrazine-1-carboximidamide (**10d**)*: Yellow solid (100 mg, 67%); mp 141–143 °C; ^{1}H NMR (DMSO-d_6) δ: 8.30 (s, 1H), 8.25 (d, J = 8.4 Hz, 2H), 7.95 (d, J = 8.4 Hz, 2H), 7.83 (t, J = 8.4 Hz, 2H), 7.78 (d, J = 8.4 Hz, 2H), 7.55 (d, J = 8.4 Hz, 2H), 5.84 (brs, 2H), 5.69 (brs, 2H), 2.69 (s, 3H), 2.26 (s, 3H); ^{13}C NMR (DMSO-d_6); δ 160.2, 155.7, 152.9, 148.7, 140.5, 138.1, 137.3, 135.5, 133.8, 132.8, 129.0, 128.7, 127.9, 126.7, 125.4, 117.5, 25.3, 17.5; HPLC purity 100% (acetonitrile-3% TEA, 1 : 4).

*2-(1-(2-(4-(Benzofuran-2-yl)phenyl)-4-methyl-thiazol-5-yl) ethylidene)hydrazine-1-carboximidamide (**11d**)*: Yellow solid (90 mg, 62%); mp 136–138 °C; ^{1}H NMR (DMSO-d_6) δ: 8.26 (d, J = 8.4 Hz, 2H), 8.04 (d, J = 8.4 Hz, 2H), 7.80 (d, J = 8.4 Hz, 1H), 7.70 (d, J = 8.4 Hz, 1H), 7.68 (s, 1H), 7.57 (t, J = 8.4 Hz, 1H), 7.35 (t, J = 8.2 Hz, 1H), 5.81 (brs, 2H), 5.62 (brs, 2H), 2.67 (s, 3H), 2.25 (s, 3H); ^{13}C NMR (DMSO-d_6); δ 160.2, 155.3, 154.8, 152.5, 139.1, 137.1, 136.1, 135.7, 130.3, 129.3, 127.4, 125.2, 123.8, 121.7, 117.6, 111.6, 103.0, 25.3, 17.5; HPLC purity 98.8% (acetonitrile-3% TEA, 1 : 4).

*2-(1-(2-(4-(Benzo[b]thiophen-2-yl)phenyl)-4-methylthiazol-5-yl) ethylidene)hydrazine-1-carboximidamide (**12d**)*: Yellow solid (96 mg, 63%); mp 132–134 °C; ^{1}H NMR (DMSO-d_6) δ: 8.21 (s, 1H), 8.01–7.78 (m, 8H), 5.77 (brs, 2H), 5.60 (brs, 2H), 2.63 (s, 3H), 2.35 (s, 3H); ^{13}C NMR (DMSO-d_6); δ 160.2, 155.7, 152.5, 148.5, 143.2, 140.9, 139.1, 137.1, 135.7, 134.1, 127.5, 126.8, 125.3, 124.3, 120.8, 117.5, 25.3, 17.5; HPLC purity 97.6% (acetonitrile-3% TEA, 1 : 4).

*2-(1-(2-(4-(Furan-2-yl)phenyl)-4-methylthiazol-5-yl)ethylidene) hydrazine-1-carboximidamide (**13d**)*: Beige solid (90 mg, 71%); mp 122–124 °C; ^{1}H NMR (DMSO-d_6) δ: 7.94 (d, J = 8.4 Hz, 2H), 7.77 (d, J = 8.4 Hz, 2H), 7.62 (d, J = 8.4 Hz, 2H), 7.19 (t, J = 6.2 Hz, 1H), 5.78 (brs, 2H), 5.67 (brs, 2H), 2.61 (s, 3H), 2.33 (s, 3H); ^{13}C NMR (DMSO-d_6); δ 162.3, 160.1, 148.3, 145.0, 143.1, 140.5, 135.6, 133.8, 132.1, 126.6, 126.5, 125.7, 109.0, 18.6, 16.5; HPLC purity 96.5% (acetonitrile-3% TEA, 1 : 4).

*2-(1-(2-(4-(Furan-3-yl)phenyl)-4-methylthiazol-5-yl)ethylidene) hydrazine-1-carboximidamide (**14d**)*: Beige solid (84 mg, 66%); mp 120–122 °C; ^{1}H NMR (DMSO-d_6) δ: 8.30 (s, 1H), 7.92 (d, J = 8.2 Hz, 2H), 7.78 (d, J = 8.2 Hz, 1H), 7.73 (d, J = 8.4 Hz, 2H), 7.03 (d, J = 6.4 Hz, 1H), 5.77 (brs, 2H), 5.66 (brs, 2H), 2.60 (s, 3H), 2.32 (s, 3H); ^{13}C NMR (DMSO-d_6); δ 162.3, 160.1, 148.3, 145.0, 143.1, 140.5, 135.6, 133.8, 132.1, 126.6, 126.5, 125.7, 109.0, 18.6, 16.5; HPLC purity 97% (acetonitrile-3% TEA, 1 : 4).

*2-(1-(4-Methyl-2-(4-(thiophen-2-yl)phenyl)thiazol-5-yl) ethylidene)hydrazine-1-carboximidamide (**15d**)*: Yellow solid (90 mg, 76%) mp = 120–122 °C; ^{1}H NMR (DMSO-d_6) δ: 7.94 (d, J = 8 Hz, 2H), 7.76 (d, J = 8 Hz, 2H), 7.63–7.60 (m, 2H), 7.19–7.17 (m, 1H), 5.79 (brs, 2H), 5.67 (brs, 2H), 2.60 (s, 3H), 2.32 (s, 3H); ^{13}C NMR (DMSO-d_6) δ: 160.2, 158.1, 148.4, 142.9, 135.9, 133.6, 131.9, 129.2, 126.8, 126.3, 124.9, 18.6, 16.5; MS (m/z) 355; HPLC purity 96.2% (acetonitrile-3% TEA, 1 : 4).

*2-(1-(4-Methyl-2-(4-(thiophen-3-yl)phenyl)thiazol-5-yl) ethylidene)hydrazine-1-carboximidamide (**16d**)*: Yellow solid (102 mg, 88%) mp = 123–125 °C; ^{1}H NMR (DMSO-d_6) δ: 7.97 (s, 1H), 7.93 (d, J = 8 Hz, 2H), 7.83 (d, J = 8 Hz, 2H), 7.67 (d, J = 8 Hz, 1H), 7.63 (d, J = 8 Hz, 1H), 5.79 (brs, 2H), 5.67 (brs, 2H), 2.60 (s, 3H), 2.32 (s, 3H); ^{13}C NMR (DMSO-d_6) δ: 162.2, 160.1, 148.3, 143.1, 141.0, 136.7, 135.7, 132.2, 127.8, 127.0, 126.6, 126.5, 122.2, 18.6, 16.5; MS (m/z) 355; HPLC purity 94.7% (acetonitrile-3% TEA, 1 : 4).

*(1-(4-Methyl-2-(4-(5-methylthiophen-3-yl)phenyl)thiazol-5-yl) ethylidene)hydrazine-1-carboximidamide (**17d**)*: Yellow solid (105 mg, 89%) mp = 120–122 °C; ^{1}H NMR (DMSO-d_6) δ: 7.91 (d, J = 8 Hz, 2H), 7.78 (d, J = 8 Hz, 2H), 7.71 (s, 1H), 7.32 (s, 1H), 5.79 (brs, 2H), 5.68 (brs, 2H), 2.60 (s, 3H), 2.42 (s, 3H), 2.32 (s, 3H); ^{13}C NMR (DMSO-d_6) δ: 162.2, 160.2, 148.3, 143.0, 140.8, 140.6, 136.9, 135.7, 132.1, 126.8, 126.6, 124.8, 120.0, 18.6, 16.5, 15.5; MS (m/z) 369; HPLC purity 97% (acetonitrile-3% TEA, 1 : 4).

*2-(1-(2-(4-(4,5-Dimethylthiophen-3-yl)phenyl)-4-methylthiazol-5-yl)ethylidene)hydrazine-1-carboximidamide (**18d**)*: Yellow solid (106 mg, 90%) mp = 123–125 °C; ^{1}H NMR (DMSO-d_6) δ: 7.94 (d, J = 8 Hz, 2H), 7.49 (d, J = 8 Hz, 2H), 7.29 (s, 1H), 5.78 (brs, 2H), 5.69 (brs, 2H), 2.60 (s, 3H), 2.38 (s, 3H), 2.32 (s, 3H), 2.12 (s, 3H); ^{13}C NMR (DMSO-d_6) δ: 162.3, 160.1, 148.4, 143.1, 142.6, 138.9, 135.7, 134.1, 132.1, 131.4, 129.4, 126.2, 119.9, 18.6, 16.5, 13.9, 13.5; MS (m/z) 383; HPLC purity 98.9% (acetonitrile-3% TEA, 1 : 4).

*2-{1-[4-Methyl-2-(4-(5-(N-methylsulfamoyl)thiophen-2-yl) phenyl)thiazol-5-yl]ethylidene}hydrazine-1-carboximidamide (**19d**)*: Yellow solid (80 mg, 70%) mp = 129–131 °C; ^{1}H NMR (DMSO-d_6) δ: 7.97 (d, J = 8.4 Hz, 2H), 7.84 (d, J = 8.4 Hz, 2H), 7.71 (brs, 1H), 7.68 (d, J = 4 Hz, 1H), 7.60 (d, J = 4 Hz, 1H), 5.78 (brs, 2H), 5.67 (brs, 2H), 2.60 (s, 3H), 2.56 (s, 3H), 2.32 (s, 3H); ^{13}C NMR (DMSO-d_6) δ: 161.5, 160.2, 148.5, 148.4, 142.9, 139.6, 136.4, 133.9, 133.6, 133.2, 126.98, 126.94, 125.0, 29.3, 18.6, 16.4; MS (m/z) 448.5; HPLC purity 95.9% (acetonitrile-3% TEA, 1 : 4).

*2-(1-(2-(4-(5-(N-Ethylsulfamoyl)thiophen-2-yl)phenyl)-4-methylthiazol-5-yl)ethylidene)hydrazine-1-carboximidamide (**20d**)*: Yellow solid (83 mg, 73%) mp = 130–132 °C; ^{1}H NMR (DMSO-d_6) δ: 7.97 (d, J = 8.4 Hz, 2H), 7.90 (brs, 1H), 7.83 (d, J = 8.4 Hz, 2H), 7.66 (d, J = 4 Hz, 1H), 7.60 (d, J = 4 Hz, 1H), 5.89 (brs, 4H), 2.98 (q, J = 6.8 Hz, 2H), 2.60 (s, 3H), 2.33 (s, 3H), 1.06 (t, J = 6.8 Hz, 3H); ^{13}C NMR (DMSO-d_6) δ: 161.7, 159.9, 148.9, 148.3, 143.3, 140.9, 136.0, 133.8, 133.7, 132.9, 126.9, 126.6, 125.0, 38.3, 18.6, 16.6, 15.1; MS (m/z) 462.6; HPLC purity 98.9% (acetonitrile-3% TEA, 1 : 4).

*2-{1-[2-(4-(5-(N-Isopropylsulfamoyl)thiophen-2-yl)phenyl)-4-methylthiazol-5-yl]ethylidene}hydrazine-1-carboximidamide (**21d**)*: Yellow solid (77 mg, 68%) mp = 133–135 °C; ^{1}H NMR (DMSO-d_6) δ: 7.97 (d, J = 8.4 Hz, 2H), 7.91 (brs, 1H), 7.84 (d, J = 8.4 Hz, 2H), 7.66 (d, J = 4 Hz, 1H), 7.60 (d, J = 4 Hz, 1H), 5.84 (brs, 2H), 5.73 (brs, 2H), 3.43–3.39 (m, 1H), 2.60 (s, 3H), 2.31 (s, 3H), 1.04 (d, J = 6.4 Hz, 6H); ^{13}C NMR (DMSO-d_6) δ: 161.5, 160.3, 148.5, 148.1, 142.8, 142.3, 136.4, 133.8, 133.7, 132.8, 127.2, 126.9, 124.9, 46.1, 23.6, 18.6, 16.4; MS (m/z) 476.6; HPLC purity 91% (acetonitrile-3% TEA, 1 : 4).

*2-{1-[2-(4-(5-(N-Butylsulfamoyl)thiophen-2-yl)phenyl)-4-methylthiazol-5-yl]ethylidene}hydrazine-1-carboximidamide (**22d**)*: Yellow solid (79 mg, 70%) mp = 136–138 °C; ^{1}H NMR (DMSO-d_6) δ: 7.97 (d, J = 8.4 Hz, 2H), 7.90 (brs, 1H), 7.84 (d, J = 8.4 Hz, 2H), 7.67 (d, J = 4 Hz, 1H), 7.60 (d, J = 4 Hz, 1H), 5.86 (brs, 4H), 2.90 (t, J = 6.4 Hz, 2H), 2.60 (s, 3H), 2.33 (s, 3H), 1.43 (m, 2H), 1.31 (m, 2H), 0.85 (t, J = 7.2 Hz, 3H); ^{13}C NMR (DMSO-d_6) δ: 161.6, 159.9, 148.8, 148.2, 143.2, 141.0, 136.1, 133.8, 133.7, 132.9, 127.2, 126.9, 125.4, 42.9, 31.4, 19.7, 18.6, 16.6, 13.9; MS (m/z) 490; HPLC purity 95.4% (acetonitrile-3% TEA, 1 : 4).

*2-{1-[4-Methyl-2-(4-(5-(N-(pentan-2-yl)sulfamoyl)thiophen-2-yl) phenyl)thiazol-5-yl]ethylidene}hydrazine-1-carboximidamide (**23d**)*: Yellow solid (83 mg, 73%) mp = 136–138 °C; ^{1}H NMR (DMSO-d_6) δ: 7.97 (d, J = 8.4 Hz, 2H), 7.89 (brs, 1H), 7.83 (d, J = 8.4 Hz, 2H), 7.65 (d, J = 4 Hz, 1H), 7.59 (d, J = 4 Hz, 1H), 5.83 (brs, 4H), 3.37–3.28 (m, 1H), 2.60 (s, 3H), 2.32 (s, 3H), 1.33–1.21 (m, 4H), 0.98–0.97 (m, 3H), 0.79–0.76 (m, 3H); ^{13}C NMR (DMSO-d_6) δ: 161.6, 160.0, 148.7, 148.0, 143.2, 142.6, 136.2, 133.8, 133.7, 132.7, 126.95, 126.92, 124.9, 49.8, 42.6, 21.5, 18.8, 18.6, 16.5, 14.1; MS (m/z) 504.6; HPLC purity 98.13% (acetonitrile-3% TEA, 1 : 4).

*2-{1-[2-(4-(5-(N-Hexylsulfamoyl)thiophen-2-yl)phenyl)-4-methylthiazol-5-yl]ethylidene}hydrazine-1-carboximidamide (**24d**)*: Yellow solid (87 mg, 77%) mp = 139–141 °C; ^{1}H NMR (DMSO-d_6) δ: 7.97 (d, J = 8.4 Hz, 2H), 7.88 (brs, 1H), 7.83 (d, J = 8.4 Hz, 2H), 7.66 (d, J = 4 Hz, 1H), 7.59 (d, J = 4 Hz, 1H), 5.79 (brs, 2H), 5.71 (brs, 2H), 2.89 (t, J = 8 Hz, 2H), 2.60 (s, 3H), 2.32 (s, 3H), 1.43–1.37 (m, 2H), 1.28–1.16 (m, 6H), 0.83–0.80 (m, 3H); ^{13}C NMR (DMSO-d_6) δ: 161.5, 160.2, 148.5, 148.2, 143.0, 141.0, 136.3, 133.8, 133.7, 132.9, 126.98, 126.94, 124.9, 43.2, 31.2, 29.2, 26.1, 22.4, 18.6, 16.5, 14.3; MS (m/z) 518.7; HPLC purity 97.7% (acetonitrile-3% TEA, 1 : 4).

*2-{1-[2-(4-(5-(N,N-Diethylsulfamoyl)thiophen-2-yl)phenyl)-4-methylthiazol-5-yl]ethylidene}hydrazine-1-carboximidamide (**25d**)*: Yellow solid (80 mg, 70%) mp = 135–137 °C; ^{1}H NMR (DMSO-d_6) δ: 7.97 (d, J = 8.4 Hz, 2H), 7.85 (d, J = 8.4 Hz, 2H), 7.70 (d, J = 4 Hz, 1H), 7.67 (d, J = 4 Hz, 1H), 5.78 (brs, 2H), 5.7 (brs, 2H), 3.25 (q, J = 7.2 Hz, 4H), 2.60 (s, 3H), 2.32 (s, 3H), 1.39 (t, J = 7.2 Hz, 6H); ^{13}C NMR (DMSO-d_6) δ: 161.4, 160.2, 148.7, 148.5, 143.0, 139.0, 136.4, 133.9, 133.5, 133.3, 127.0, 126.9, 125.2, 42.9, 18.6, 16.5, 14.6; MS (m/z) 490.6; HPLC purity 95.7% (acetonitrile-3% TEA, 1 : 4).

4.2. Biological assays

4.2.1. Bacterial strains, media, cell lines and reagents. Clinical isolates used in this study were obtained from the Biodefense and Emerging Infections Research Resources Repository (BEI Resources) and the American Type Culture Collection (ATCC). Cation-adjusted Mueller Hinton broth (CAMHB), tryptic soy broth (TSB) and tryptic soy agar (TSA) were purchased from Becton, Dickinson and Company (Cockeysville, MD, USA), and the human colorectal adenocarcinoma (Caco-2) cell line was purchased from ATCC (Manassas, VA, USA). Dulbecco's Modified Eagle Medium (DMEM) was obtained from Sigma-Aldrich (St. Louis, MO, USA). Fetal bovine serum (FBS) and phosphate-buffered saline (PBS) were purchased from Corning (Manassas, VA, USA). Linezolid and vancomycin were purchased from Chem-Impex International (Wood Dale, IL,

USA). Compounds were synthesized from commercial sources in our laboratory and prepared in stock solutions in DMSO.

4.2.2. MICs of phenylthiazole compounds against *S. aureus* clinical isolates. MICs of phenylthiazole compounds were determined against staphylococcal clinical isolates using the broth microdilution method, as described previously.[36] Briefly, a 0.5 McFarland standard bacterial solution was prepared and diluted in cation-adjusted Mueller-Hinton broth to achieve a bacterial concentration of about 5×10^5 CFU mL^{-1} and seeded in 96-well plates. Serial dilutions of test agents were incubated with bacteria aerobically at 37 °C for 18–20 h. MICs were determined as the lowest concentrations of test agents that could completely inhibited the bacterial growth.[37]

4.2.3. MICs of phenylthiazole compounds against other clinically important Gram-positive bacteria. Phenylthiazole compounds were examined against a panel of clinically relevant Gram-positive bacterial pathogens, including *Streptococcus pneumoniae*, vancomycin-resistant *Enterococcus faecium* and *Enterococcus faecalis* (VRE), and *Listeria monocytogenes* and *Clostridioides difficile*, as described in previous reports.[38–42] Streptococcal strains were grown overnight at 37 °C on blood agar plates in the presence of 5% CO_2. Enterococcal strains and *L. monocytogenes* were grown aerobically overnight on tryptone soy agar plates at 37 °C. *C. difficile* was grown anaerobically onto brain heart infusion supplemented (BHIS) agar at 37 °C for 48 hours. Afterwards, a bacterial solution equivalent to 0.5 McFarland standard was prepared and diluted in tryptone soya broth (for *E. faecalis*, *E. faecium*, and *L. monocytogenes*) to achieve a bacterial concentration of about 5×10^5 CFU mL^{-1} and seeded in 96-well plates. The 0.5 McFarland bacterial solution of streptococcal strains was diluted in cation-adjusted Mueller-Hinton broth (CAMHB) supplemented with 5% lysed horse blood, to achieve a bacterial concentration of about 5×10^5 CFU mL^{-1}. *C. difficile* was diluted in BHIS broth to achieve a bacterial concentration of about 5×10^5 CFU mL^{-1}. Compounds and control drugs were added in the first row of 96-well plates and serially diluted along the plates. Plates were then incubated aerobically at 37 °C for 18–20 hours (except for *S. pneumoniae*, which was incubated at 37 °C in the presence of 5% CO_2 for 18–20 hours, and *C. difficile* which was incubated anaerobically at 37 °C for 48 hours). MICs reported in Table 2 are the minimum concentrations of the compounds and control drugs that completely inhibited the visual growth of bacteria.

4.2.4. *In vitro* cytotoxicity analysis of phenylthiazole compounds against Caco-2 cells. Phenylthiazole compounds were assayed (at concentrations of 8, 16, and 32) against a human colorectal adenocarcinoma (Caco-2) cell line to determine the potential toxic effect to mammalian cells *in vitro*. Briefly, cells were cultured in Dulbecco's Modified Eagle Medium (DMEM) supplemented with 10% fetal bovine serum (FBS), non-essential amino acids (1X), penicillin-streptomycin at 37 °C with 5% CO_2. Compounds were added and serially diluted. Control cells received DMSO (the solvent of the compounds) alone at a concentration equal to that in compound-treated wells to determine the baseline measure of the cytotoxic impact of the compounds. The cells were incubated with the compounds (in triplicate) in a 96-well plate at 37 °C with 5% CO_2 for 24 hours. The assay reagent MTS 3-(4,5-dimethylthiazol-2-yl)-5-(3-carboxymethoxyphenyl)-2-(4-sulfophenyl)-2*H*-tetrazolium (Promega, Madison, WI, USA) was subsequently added and the plate was incubated for four hours. Absorbance readings (at OD_{490}) were recorded using a kinetic microplate reader (Molecular Devices, Sunnyvale, CA, USA). The quantity of viable cells after treatment with each compound was expressed as a percentage of the viability of DMSO-treated control cells (average of triplicate wells ± standard deviation).

4.2.5. Time-kill kinetics assay of compounds against MRSA. MRSA NRS123 cells in logarithmic growth phase were diluted to ~10^6 CFU mL^{-1} and exposed to concentrations equivalent to 5 × MIC (in triplicate) of phenylthiazole compounds, linezolid and vancomycin in tryptic soy broth. DMSO (solvent for compounds) served as a negative control. Aliquots were collected from each treatment after 0, 2, 4, 6, 8, 12 and 24 hours of incubation at 37 °C and subsequently serially diluted in PBS. Bacteria were then transferred to tryptic soy agar plates and incubated at 37 °C for 18–20 hours before viable CFU mL^{-1} was determined (Fig. 2).

4.2.6. Multi-step resistance study for phenylthiazole compounds against MRSA. The broth microdilution assay was utilized to determine the MIC of phenylthiazole compounds and rifampicin exposed to MRSA USA400 (NRS123) for consecutive passages. Resistance was classified as a greater than four-fold increase in the initial MIC, as reported earlier.[43]

4.2.7. Murine skin infection model. Animal procedures were approved by the Research Ethics Committee of the Faculty of Pharmacy, Cairo University [approval no. (MI 2868)] following the Guide for the Care and Use of Laboratory Animals published by the Institute of Laboratory Animal Research (USA). The murine skin infection was performed as previously described.[44,45] Briefly, three groups ($n = 5$) of 6 to 8 weeks-old female BALB/c mice, 18–20 g each, were included in the experiment. Mice were kept in their cages and given food and water *ad libitum*. One day prior to the infection, mice backs were shaved using an electric hair clipper. The following day, mice were anesthetized using 2,2,2-tribromoethanol (25 mg mL^{-1}) and injected subcutaneously with 100 μL containing 2×10^9 CFU of MRSA USA300, suspended in 0.5% hydroxypropyl methylcellulose (HPMC) in sterile pyrogen-free saline. Seventy-two hours post-infection (day 3), the infection site was treated with either petroleum jelly (PG), petroleum jelly containing 2% compound **15d**, or the commercially available topical ointment containing 2% fusidic acid. Topical treatments were applied twice daily for four consecutive days. The weights of the mice were recorded daily and monitored throughout the experiment. Twenty-four hours after the last treatment dose, mice were euthanized with an overdose of anesthesia. A skin patch equivalent to ~1.5 cm^2, surrounding the lesion site, was aseptically excised from the back of each mouse. In addition, the mice were dissected, and their spleens were excised to assess the systemic dissemination of the infection. The skin patch was homogenized in 1 mL pyrogen-free saline, while the spleen was homogenized in 0.5 mL saline. The homogenates were then serially diluted and plated on mannitol salt agar (MSA) plates. Plates were incubated at 37 °C overnight and the grown colonies

were counted to determine the CFU mL^{-1} counts. Statistical analysis was performed using GraphPad Prism (version 9.0) (GraphPad Software, Inc., USA), applying the one-way ANOVA, followed by Tukey's multiple comparisons test.

Conflicts of interest

All authors declare that they have no conflict of interest.

Acknowledgements

This paper is based on work supported by Science, Technology & Innovation Funding Authority (STDF) under grant number (43229) young researcher.

References

1 G. M. Knight, R. E. Glover, C. F. McQuaid, I. D. Olaru, K. Gallandat, Q. J. Leclerc, N. M. Fuller, S. J. Willcocks, R. Hasan and E. van Kleef, *Elife*, 2021, **10**, e64139.
2 C. L. Ventola, *Pharm. Ther.*, 2015, **40**, 277.
3 C. J. Murray, K. S. Ikuta, F. Sharara, L. Swetschinski, G. R. Aguilar, A. Gray, C. Han, C. Bisignano, P. Rao and E. Wool, *Lancet*, 2022, **399**, 629–655.
4 P. Mazumder, A. Kalamdhad, G. T. Chaminda and M. Kumar, *Case Stud. Chem. Environ. Eng.*, 2021, **3**, 100093.
5 B. J. Langford, M. So, V. Leung, S. Raybardhan, J. Lo, T. Kan, F. Leung, D. Westwood, N. Daneman and D. R. MacFadden, *Clin. Microbiol. Infect.*, 2022, **28**, 491–501.
6 R. J. Fair and Y. Tor, *Perspect. Med. Chem.*, 2014, **6**, S14459.
7 B. Tornimbene, S. Eremin, M. Escher, J. Griskeviciene, S. Manglani and C. L. Pessoa-Silva, *Lancet Infect. Dis.*, 2018, **18**, 241–242.
8 E. F. Kong, J. K. Johnson and M. A. Jabra-Rizk, *PLoS Pathog.*, 2016, **12**, e1005837.
9 P. Rodríguez-López, V. Filipello, P. A. Di Ciccio, A. Pitozzi, S. Ghidini, F. Scali, A. Ianieri, E. Zanardi, M. N. Losio and A. C. Simon, *Foods*, 2020, **9**, 1141.
10 R. H. Deurenberg, C. Vink, S. Kalenic, A. Friedrich, C. Bruggeman and E. Stobberingh, *Clin. Microbiol. Infect.*, 2007, **13**, 222–235.
11 G. J. Moran, A. Krishnadasan, R. J. Gorwitz, G. E. Fosheim, L. K. McDougal, R. B. Carey and D. A. Talan, *N. Engl. J. Med.*, 2006, **355**, 666–674.
12 B. W. Frazee, J. Lynn, E. D. Charlebois, L. Lambert, D. Lowery and F. Perdreau-Remington, *Ann. Emerg. Med.*, 2005, **45**, 311–320.
13 S. K. Fridkin, J. C. Hageman, M. Morrison, L. T. Sanza, K. Como-Sabetti, J. A. Jernigan, K. Harriman, L. H. Harrison, R. Lynfield and M. M. Farley, *N. Engl. J. Med.*, 2005, **352**, 1436–1444.
14 S. Kishore, D. Verma and M. Siddique, *J. Clin. Diagn. Res.*, 2014, **8**, DC12.
15 H. T. Nour El-Din, A. S. Yassin, Y. M. Ragab and A. M. Hashem, *Infect. Drug Resist.*, 2021, 1557–1571.
16 A. W. Karchmer and A. S. Bayer, *Clin. Infect. Dis.*, 2008, **46**, S342–S343.
17 H. Mohammad, A. S. Mayhoub, A. Ghafoor, M. Soofi, R. A. Alajlouni, M. Cushman and M. N. Seleem, *J. Med. Chem.*, 2014, **57**, 1609–1615.
18 M. M. Elsebaei, H. Mohammad, A. Samir, N. S. Abutaleb, A. B. Norvil, A. R. Michie, M. M. Moustafa, H. Samy, H. Gowher and M. N. Seleem, *Eur. J. Med. Chem.*, 2019, **175**, 49–62.
19 N. Brown, *Mol. Inf.*, 2014, **33**, 458–462.
20 K. Okamoto, A. Ishikawa, R. Okawa, K. Yamamoto, T. Sato, S.-i. Yokota, K. Chiba and S. Ichikawa, *Bioorg. Med. Chem.*, 2022, **55**, 116556.
21 M. M. Elsebaie, H. T. N. El-Din, N. S. Abutaleb, A. A. Abuelkhir, H.-W. Liang, A. S. Attia, M. N. Seleem and A. S. Mayhoub, *Eur. J. Med. Chem.*, 2022, **234**, 114204.
22 A. M. Sayed, N. S. Abutaleb, A. Kotb, H. G. Ezzat, M. N. Seleem, A. S. Mayhoub and M. M. Elsebaie, *J. Heterocycl. Chem.*, 2023, **60**, 134–144.
23 M. A. Seleem, A. M. Disouky, H. Mohammad, T. M. Abdelghany, A. S. Mancy, S. A. Bayoumi, A. Elshafeey, A. El-Morsy, M. N. Seleem and A. S. Mayhoub, *J. Med. Chem.*, 2016, **59**, 4900–4912.
24 H. Mohammad, P. N. Reddy, D. Monteleone, A. S. Mayhoub, M. Cushman and M. N. Seleem, *Eur. J. Med. Chem.*, 2015, **94**, 306–316.
25 M. M. Elsebaei, N. S. Abutaleb, A. A. Mahgoub, D. Li, M. Hagras, H. Mohammad, M. N. Seleem and A. S. Mayhoub, *Eur. J. Med. Chem.*, 2019, **182**, 111593.
26 G. A. Molander, S. L. Trice and S. M. Kennedy, *J. Org. Chem.*, 2012, **77**, 8678–8688.
27 J. Yu, A. Ciancetta, S. Dudas, S. Duca, J. Lottermoser and K. A. Jacobson, *J. Med. Chem.*, 2018, **61**, 4860–4882.
28 M. Carrel, E. N. Perencevich and M. Z. David, *Emerging Infect. Dis.*, 2015, **21**, 1973.
29 G. R. Golding, P. N. Levett, R. R. McDonald, J. Irvine, B. Quinn, M. Nsungu, S. Woods, M. Khan, M. Ofner-Agostini and M. R. Mulvey, *Emerging Infect. Dis.*, 2011, **17**, 722.
30 U. Seybold, E. V. Kourbatova, J. G. Johnson, S. J. Halvosa, Y. F. Wang, M. D. King, S. M. Ray and H. M. Blumberg, *Clin. Infect. Dis.*, 2006, **42**, 647–656.
31 B. A. Diep, H. A. Carleton, R. F. Chang, G. F. Sensabaugh and F. Perdreau-Remington, *J. Infect. Dis.*, 2006, **193**, 1495–1503.
32 P. Peters, J. Brooks, B. Limbago, H. Lowery, S. McAllister, R. Mindley, G. Fosheim, R. Gorwitz, J. Guest and J. Hageman, *Epidemiol. Infect.*, 2011, **139**, 998–1008.
33 G. Zhen, G. Zeng, K. Jiang, F. Wang, X. Cao and B. Yin, *Chem.–Eur. J.*, 2023, **29**, e202203217.
34 A. U. Meyer, A. L. Berger and B. König, *Chem. Commun.*, 2016, **52**, 10918–10921.
35 L. Zhou, T. Kawate, X. Liu, Y. B. Kim, Y. Zhao, G. Feng, J. Banerji, H. Nash, C. Whitehurst and S. Jindal, *Bioorg. Med. Chem.*, 2012, **20**, 750–758.
36 M. A. Wikler, *CLSI (NCCLS)*, 2006, 26, pp. M7–A7.
37 N. S. Abutaleb, A. Elkashif, D. P. Flaherty and M. N. Seleem, *Antimicrob. Agents Chemother.*, 2021, **65**, e01715–e01720.
38 N. S. Abutaleb and M. N. Seleem, *Antimicrob. Agents Chemother.*, 2020, **64**, e02115–e02119.

39 N. S. Abutaleb and M. N. Seleem, *Sci. Rep.*, 2020, **10**, 1–8.
40 N. S. Abutaleb, A. E. Elhassanny, D. P. Flaherty and M. N. Seleem, *PeerJ*, 2021, **9**, e11059.
41 N. S. Abutaleb and M. N. Seleem, *Int. J. Antimicrob. Agents*, 2020, **55**, 105828.
42 N. S. Abutaleb, A. E. Elhassanny, A. Nocentini, C. S. Hewitt, A. Elkashif, B. R. Cooper, C. T. Supuran, M. N. Seleem and D. P. Flaherty, *J. Enzyme Inhib. Med. Chem.*, 2022, **37**, 51–61.
43 H. Mohammad, W. Younis, H. G. Ezzat, C. E. Peters, A. AbdelKhalek, B. Cooper, K. Pogliano, J. Pogliano, A. S. Mayhoub and M. N. Seleem, *PLoS One*, 2017, **12**, e0182821.
44 C. W. Tseng, M. Sanchez-Martinez, A. Arruda and G. Y. Liu, *J. Vis. Exp.*, 2011, **48**, 2528.
45 M. Hagras, N. S. Abutaleb, N. M. Elhosseiny, T. M. Abdelghany, M. Omara, M. M. Elsebaei, M. Alhashimi, A. B. Norvil, M. I. Gutay and H. Gowher, *ACS Infect. Dis.*, 2020, **6**, 2887–2900.